

Velocity Distribution and the Effect of Wall Roughness in Granular Poiseuille Flow

K. C. Vijayakumar and Meheboob Alam*

Engineering Mechanics Unit, Jawaharlal Nehru Center for

Advanced Scientific Research, Jakkur PO, Bangalore 560064, India

(Dated: October 26, 2018)

From event-driven simulations of a gravity-driven channel flow of inelastic hard-disks, we show that the velocity distribution function remains close to a Gaussian for a wide range densities (even when the Knudsen number is of order one) if the walls are smooth and the particle collisions are nearly elastic. For dense flows, a transition from a Gaussian to a power-law distribution for the high velocity tails occurs with increasing dissipation in the center of the channel, irrespective of wall-roughness. For a rough wall, the near-wall distribution functions are distinctly different from those in the bulk even in the quasielastic limit.

PACS numbers: 45.70.-n, 47.57.Gc

Granular materials, a collection of macroscopic particles, are important in many chemical and pharmaceutical industries as well as in geophysical contexts (avalanche, sand dune, etc.). In the rapid flow regime [1], the theory for flowing granular materials is largely based on the dense gas kinetic theory that incorporates the *inelastic* nature of particle collisions. At the heart of such gas- or liquid-state continuum theories lies the concept of ‘coarse-graining’ over distribution functions while making a transition from the particle-level properties to the macro-scale fields. Unlike the molecular fluid for which the Maxwell-Boltzmann (Gaussian/Maxwellian) distribution plays the role of the ‘equilibrium’ distribution function, however, the granular fluid does not possess any ‘equilibrium’ state [1, 2] due to the microscopic dissipation of particle collisions. However, there are ‘non-equilibrium’ (driven) steady-states for various canonical granular flow configurations for which the Gaussian distribution is the leading-order velocity distribution [2] in appropriate limits. A systematic study of distribution functions is, therefore, of interest from the viewpoint of

* Author to whom correspondence should be addressed: Electronic Address: meheboob@jncasr.ac.in; Published in *Physical Review E*, vol. 75, 051306 (2007)

developing constitutive models for granular flows as well as to pinpoint the range of validity of any adopted theory. Another important issue that needs attention is the derivation of continuum boundary conditions for granular flows [3] where it is generally assumed that the distribution function in the near wall-region is the same as that in the bulk which is unlikely to hold as we shall show here.

In ‘driven’ granular flows, the deviation of velocity distribution from a Gaussian has been studied through theory [2, 4], simulation [5, 6] and experiment [7, 8, 9]. In Ref. [5] it has been shown that the velocity fluctuations in a vibrated bed of particles follow a Gaussian distribution in the solid phase and a power-law distribution (with an exponent -3) in the fluidized phase. For the plane shear flow [2], the velocity distribution function is well fitted by an exponent of a second-order polynomial in the norm of the fluctuating velocities with angle-dependent coefficients. Theoretical works [4] for a randomly heated granular gas, based on the Boltzmann-Enskog equation, have predicted velocity distribution functions of the form $P(v) \sim \exp(-\gamma v^\alpha)$, with the exponent of high-velocity tails being $\alpha = 3/2$ which also depends on the level of inelastic dissipation. Experiments [7] for a granular gas confined between two vertical plates and driven into a steady state via vertical vibrations have shown that $\alpha \sim 1.55 \pm 0.1$, for a wide range of frequency and amplitude of vibrations. Some recent experiments [8], however, showed that the high-velocity tails cannot be described by a ‘single’ universal exponent.

In this paper we consider the ‘granular’ Poiseuille flow which is the gravity-driven flow of granular materials through a two-dimensional channel [10], focusing on the ‘rapid’ flow regime [1]. The simulated system is a channel of length L along the periodic x -direction and bounded by two plane solid walls, parallel to the x -direction, with a separation of width W (along the y -direction). The granular material, consisting of N identical rigid and smooth disks of equal mass and diameter d , is driven by gravity along the x -direction. The interactions that are allowed are instantaneous ‘dissipative’ collisions between pairs of particles and between a particle and the walls, via an event-driven algorithm [11]. The dissipative nature of particle collisions is characterized by the coefficient of normal restitution, e_n , which is the ratio between the pre- and post-collisional relative velocities of the colliding particles. There is no relative tangential velocity since the particles are assumed to be smooth. The solid walls are modeled as frictional surfaces, and a particle colliding with a wall is analogous to a particle colliding with a particle of infinite mass moving at the velocity of the wall. The frictional properties of the walls are modeled using a single parameter, the *coefficient of tangential restitution* for particle-wall collisions (β_w), which is defined as the

fraction of relative tangential momentum transmitted from a particle to the wall during a particle-wall collision. The wall-roughness is controlled by choosing a specific value of β_w : while $\beta_w = 1$ corresponds to a fully *smooth* wall, $\beta_w = 0$ corresponds to a fully *rough* wall for which the dissipation of energy at walls is maximum and there is no relative tangential slip between the particle surface and the wall upon a wall-particle collision.

Apart from the wall-roughness parameter β_w , the granular Poiseuille flow is governed by three control parameters: the average volume fraction (ν), the coefficient of normal restitution (e_n) and the channel width (W/d). It may be noted that the gravitational acceleration (g) does not appear explicitly as a control parameter since it is used as a reference scale for time ($\sqrt{W/g}$), velocity (\sqrt{Wg}) and other mean fields. In the present simulation, we have fixed $N = 900$ and $W/d = 31$ and varied the channel length (L/W) to change the average volume fraction,

$$\nu = \pi N/4 (L/W) (W/d)^2.$$

(The robustness of reported results was checked by increasing the number of particles by four-fold.) The system is initially allowed to attain a statistically steady state for which the stream-wise velocity (U_x), volume fraction (ν) and granular temperature (T), remain invariant in time, but have spatial variations along the wall-normal direction (y). All the statistics presented in this paper are computed ‘bin-wise’ by dividing the channel into 18–bins along the wall normal direction, and collecting the data in each bin over about 300000 collisions per particle after reaching the steady state. An increase in the number of bins to 31 did not alter the results; a few bins are indicated by arrows in Fig. 1(b), with $bin = 1, 18$ being located adjacent to the walls and $bin = 9, 10$ at the center of the channel. It is to be noted that $u_x = c_x - U_x(t)$ and $u_y = c_y$ are the particle fluctuating velocity in x – and y –directions, respectively, over the instantaneous mean velocity; here $U_x(t)$ and $U_x = \langle U_x(t) \rangle$ are the ‘instantaneous’ mean and ‘time-averaged’ mean streamwise velocity, respectively.

Figure 1(a) shows the probability distribution function of the fluctuating streamwise velocity (u_x) for dilute-to-dense flows ($0.015 \leq \nu \leq 0.56$) in different bins. The wall-roughness has been set to $\beta_w = 0.9$ for smooth walls, and the restitution coefficient to $e_n = 0.99$ for *quasi-elastic* particle collisions. (The distribution function of the fluctuating transverse velocity, u_y , looks similar, and hence not shown.) The local (bin-wise) distribution functions on only one-side of the channel-centerline are presented as the distributions on the other side is the same; however, in some cases, the distributions on both sides are presented when they differ. Note that

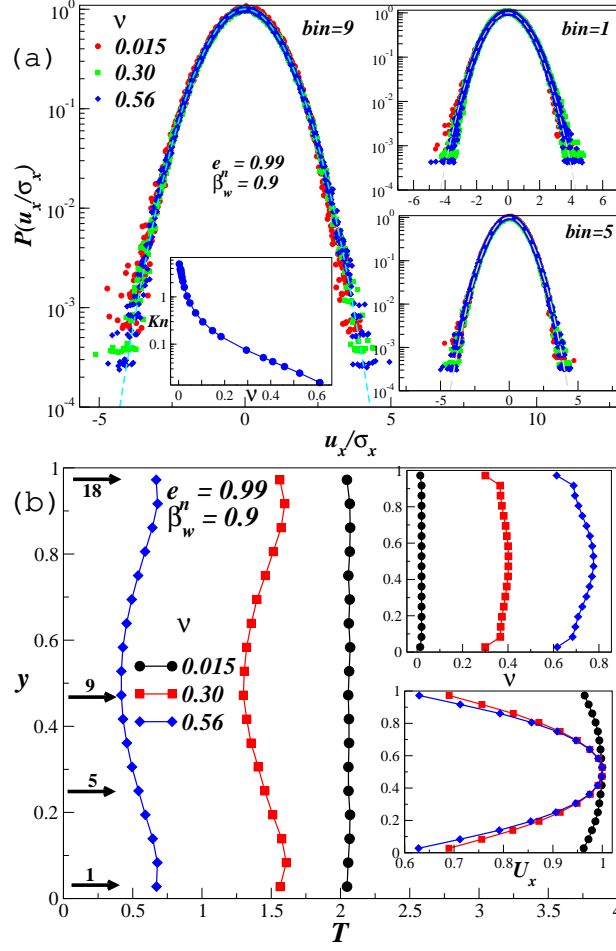


FIG. 1: (Color online) (a) Distribution function of u_x for a range of volume fractions in the quasi-elastic limit ($e_n = 0.99$) for smooth ($\beta_w = 0.9$) walls in different bins. The dashed curve indicates a Gaussian. Left inset shows the variation of Knudsen number, Kn , with volume fraction. (b) The mean velocity (U_x), granular temperature (T) and volume fraction (ν) profiles across the width of the channel for $e_n = 0.99$ and $\beta_w = 0.9$ at different volume fractions. The arrows near the left-ordinate indicate the locations of some bins.

the horizontal axis in the velocity distribution plots is scaled by $\sigma_i = \sqrt{\langle u_i^2 \rangle}$, where the index i denotes the coordinate direction, and the vertical axis has been scaled such that $P(0) = 1$. It is remarkable that the velocity distribution function in all bins remains a Gaussian for a wide range of densities ($\nu < 0.6$). This is a surprising result, especially in the dilute limit, since the Knudsen number [see left inset in Fig. 1(a)], which is the ratio between the mean free path and the channel width, $Kn = l_f/W$, increases with decreasing ν and becomes of $O(1)$ in the dilute limit, signalling the onset of rarefied flow. Even in this rarefied regime, the velocity distribution function remains a Gaussian in granular Poiseuille flow with smooth walls. From the profiles of

temperature (T), mean velocity (U_x) and volume fraction (ν) in Fig. 1(b), we observe that the mean field quantities develop considerable gradients along y -direction with increasing density (and this is more pronounced for U_x , see lower inset in Fig. 1b), however, they are almost constant over the width of a bin. The mean-field gradients do not seem to play any role in determining the form of ‘local’ velocity distribution functions as long as the walls are smooth and the particle collisions are quasielastic.

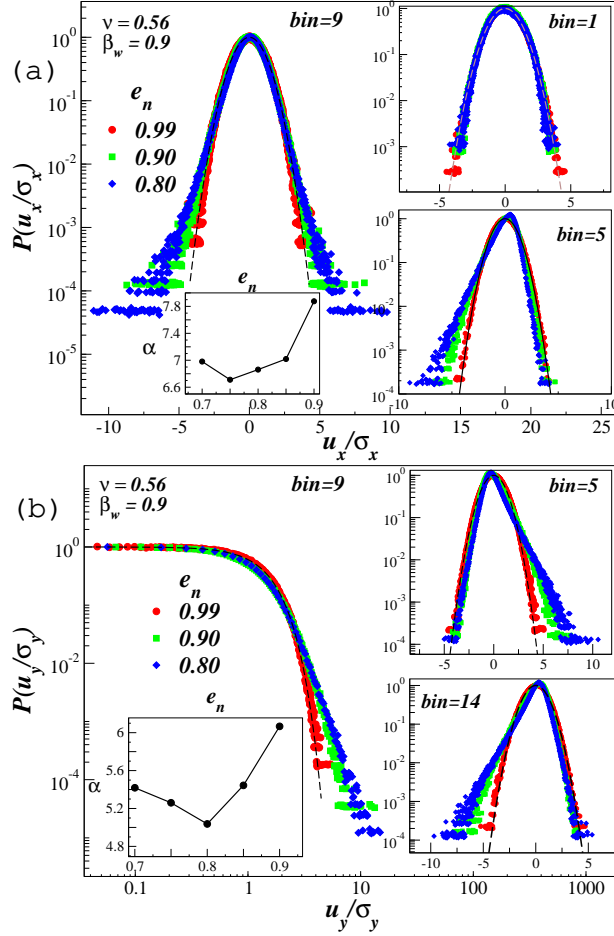


FIG. 2: (Color online) (a) Effect of restitution coefficient, e_n , on $P(u_x)$ at $\nu = 0.56$ for smooth walls ($\beta_w = 0.9$). The velocity distribution in $bin = 1$, upper inset, remains a Gaussian, the distribution in $bin = 5$, lower inset, develops asymmetric tails and the distribution in $bin = 9$ makes a transition from Gaussian to a power-law tails with increasing dissipation. Left Inset: Variation of power-law exponent, α , with e_n . (b) Same as in panel (a) but for $P(u_y)$ in log-log scale to discern the power-law behaviour.

For a dense flow, $\nu = 0.56$, with smooth walls $\beta_w = 0.9$, Fig. 2(a) shows the effect of collisional dissipation, e_n , on the form of $P(u_x)$ distribution in different bins. The velocity distribution in $bin = 1$ (adjacent to wall), the upper inset in Fig. 2(a), remains close to a Gaussian, irrespective of

the value of e_n . The $P(u_x)$ distribution in $bin = 5$ (between the wall and the channel-centerline), the lower inset in Fig. 2(a), becomes *asymmetric* with increasing dissipation, with an enhanced probability of negative velocities (negative skewness). At the center of the channel ($bin = 9$), the high velocity tails of the distribution function undergo a transition from a Gaussian to a non-Gaussian (with over-populated tails) with increasing collisional dissipation, as seen in the main panel of Fig. 2(a). The analogue of Fig. 2(a) for the fluctuating transverse velocity u_y is shown in Fig. 2(b). The transition of $P(u_y)$ in the channel-centerline is very similar to that seen in $P(u_x)$. The distribution in $bin = 1$ remains Gaussian and is not shown here, instead we include the distribution in $bin = 14$. Note that $P(u_y)$ distribution in $bin = 5$ and $bin = 14$ are mirror images since these bins are symmetrically located about the channel-centerline. The appearance of asymmetric distribution functions in two shear-layers (with increasing dissipation-level) could be a consequence of density-waves [12] in narrow shear-layers. (Within the plug-region, however, the local distribution functions are slightly affected by such asymmetries.) This issue is relegated to a future study.

For parameter values as in Fig. 2, the profiles of the mean field quantities are displayed in Fig. 3(a) which shows the emergence of a ‘plug’ around the channel-centerline (with negligible gradients in U_x , T and ν) with decreasing e_n , and two ‘shear-layers’ adjacent to two-walls with steep gradients in U_x , T and ν . To pinpoint the role of e_n on distribution functions, first we study its effect on the pair correlation function and the spatial velocity correlations. The velocity correlation function is defined as follows:

$$C_{ij} = \frac{\langle u_i(x)u_j(x + \delta x) \rangle}{\langle u_i(0)u_i(0) \rangle},$$

where the indices i, j denote the coordinate directions. In the quasielastic limit, the pair correlation function, the lower inset in Fig. 3(b), shows a liquid-like structure in all bins and the velocity correlation is close to zero (not shown). The signatures of plug-formation with increasing dissipation show up in the pair correlation function (the main panel of Fig. 3b) which indicates a transition from a liquid to a crystal-like structure in $bin = 9$ at $e_n = 0.8$. With increasing density correlation in $bin = 9$, the velocity correlation C_{xx} also becomes strong as shown in the upper inset of Fig. 3(b). (It is interesting to note that the velocity correlation is negative beyond a certain correlation length, $x/d \sim 10$, which is an indicator of circulatory-type motion [13] for the fluctuating velocity field.) At $e_n = 0.8$, the pair correlation function outside the plug region ($bin = 1, 5$) shows a gaseous structure and the C_{xx} correlation is weak/absent (see upper inset in Fig. 3b). Clearly, the enhanced density and velocity correlations around the channel-centerline are

responsible for the emergence of non-Gaussian tails with increasing dissipation (Fig. 2).

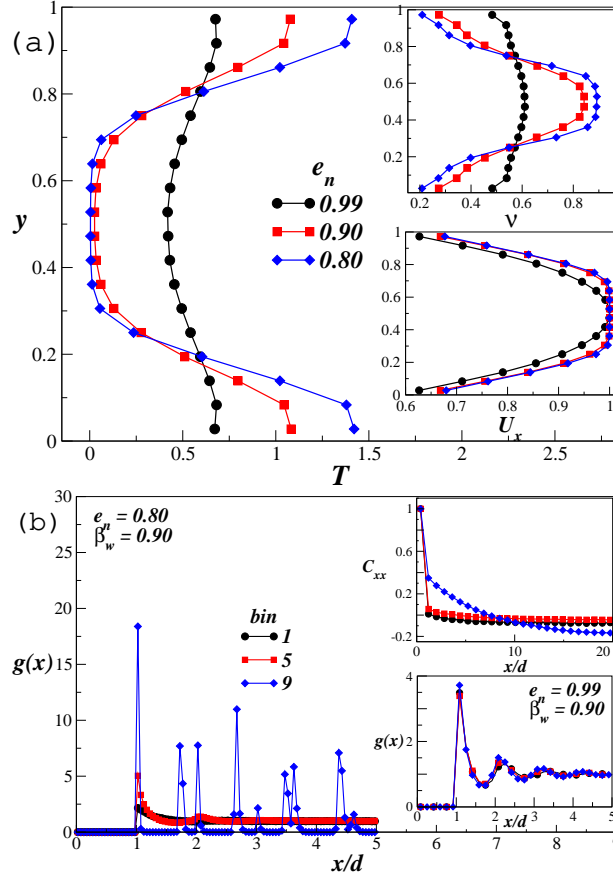


FIG. 3: (Color online) (a) Variations of U_x , T and ν along y , with parameter values as in Fig. 2. (b) Main Panel: Pair correlation function, $g(x)$, in different bins at $\nu = 0.56$ for $e_n = 0.8$ with smooth walls ($\beta_w = 0.9$). Upper Inset: Streamwise velocity correlation function (C_{xx}) with parameter values as in main panel. Lower Inset: $g(x)$ in different bins for $e_n = 0.99$ which shows a liquid-like structure.

With reference to dense flows in Fig. 2, the tails of $P(u_i)$ in the plug-region can be fitted via a power-law of the form $P(u_i) \sim u_i^{-\alpha_i}$, with a single exponent, $\alpha_x \sim 7$ and $\alpha_y \sim 5.5$, for a range of restitution coefficients, see the left insets in Figs. 2(a) and 2(b). The near-constancy of α_i for $e_n < 0.85$ is due to the fact that the density within the plug saturates to the close-packing limit ($\nu_c \sim 0.9$) for $e_n < 0.85$ and consequently the other hydrodynamic fields also remain invariant there with a further decrease in e_n . This weak-variation of α_i on e_n is also implicated in its variation with average density. A similar power-law behavior (with $\alpha \sim 2.9 - 7.4$) has recently been observed in experiments of gravity-driven channel flow [9]; however, it is difficult to make a direct comparison since the experimental geometry is different (with a sieve at the bottom) and the flow corresponds to the dense ‘quasi-static’ regime. This issue can be resolved by probing very

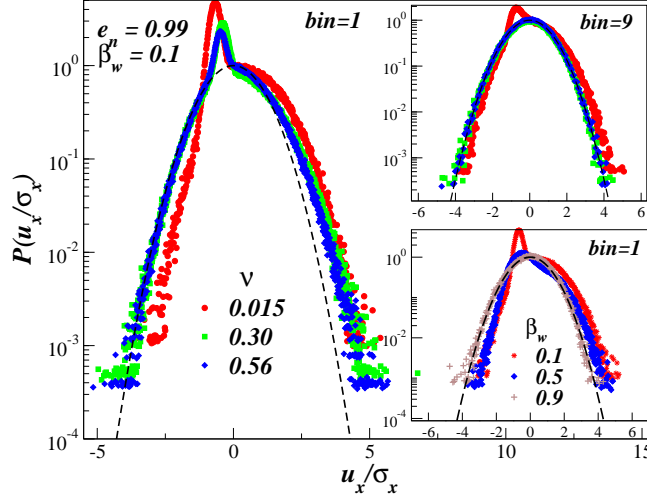


FIG. 4: (Color online) Effect of mean volume fraction on $P(u_x)$ for a rough-wall ($\beta_w = 0.1$) with $e_n = 0.99$ in $bin = 1$. Upper Inset: $bin = 9$. Lower Inset: Effect of β_w on $P(u_x)$ at $\nu = 0.015$ in $bin = 1$.

dense systems which is beyond the scope of the present paper.

The effect of wall-roughness on $P(u_x)$ is shown in Fig. 4, for a rough wall $\beta_w = 0.1$ with quasielastic collisions $e_n = 0.99$. The $P(u_x)$ distribution near the wall ($bin = 1$, the main panel) develops a single-peak asymmetric structure at all densities, with its peak being positioned at some negative velocity. Near the centerline ($bin = 9$, upper inset), however, $P(u_x)$ remains asymmetric only at low densities and becomes a Gaussian at larger densities. The corresponding $P(u_y)$ distribution (not shown) remains a Gaussian at all densities in the quasielastic limit. For dense flows with *rough* walls, both $P(u_x)$ and $P(u_y)$ develop power-law tails with decreasing e_n around the channel-centerline as in Fig. 2 for smooth walls; the wall-roughness did not influence the associated power-law exponents.

Focusing on the dilute regime ($\nu = 0.015$), the effect of β_w on $P(u_x)$ in $bin = 1$ is shown in the lower inset of Figs. 4. It is clear that the asymmetry in $P(u_x)$ diminishes with increasing wall smoothness (β_w) and becomes a Gaussian when the walls are smooth ($\beta_w = 0.9$). This wall-roughness-induced asymmetry in $P(u_x)$ is also reflected in the probability distribution of the instantaneous particle streamwise velocity c_x (not shown), with a single peak in the low velocity region for $bin = 1$ —also, $P(c_x)$ for $\nu = 0.015$ approaches a Gaussian with increased wall-smoothness. Since the particles lose significant amount of tangential velocity while colliding with a *rough* wall in comparison with their collisions with a *smooth* wall, a peak near the low velocity region is expected for rough walls. The greater the loss of tangential velocity at walls, the more is the deviation from a Gaussian, and the related asymmetry in Fig. 4 is, therefore, tied

to wall-roughness. On the whole, in dilute flows the effect of wall-roughness is felt on the local distribution functions throughout the channel, whereas for dense flows only the near-wall region is affected.

In conclusion, the local velocity distribution functions in a granular Poiseuille flow (GPF) with *smooth* walls remains Gaussian for a wide range of densities for nearly elastic collisions ($e_n \rightarrow 1$) which, in turn, suggests that the GPF (with smooth walls) could serve as a prototype ‘non-equilibrium steady state’ to derive constitutive models starting from the Boltzmann-Engskog equation. For dense flows, enhanced density correlations and the related spatial velocity correlations are responsible for the emergence of power-law tails with increasing collisional dissipation around the channel-centerline (irrespective of wall roughness) where the flow undergoes a transition from a liquid-like to a crystal-like (‘plug’) structure in the same limit. For a rough wall, the near-wall distribution functions are significantly different from those in the bulk at all densities which calls for a relook at the derivation of granular boundary conditions [3].

-
- [1] L. P. Kadanoff, Rev. Mod. Phys. **71**, 435 (1999); I. Goldhirsch, Annu. Rev. Fluid Mech. **35**, 267 (2003).
 - [2] N. Sela and I. Goldhirsch, J. Fluid Mech. **361**, 41 (1998); I. Goldhirsch and M. Tan, Phys. Fluids **8**, 1752 (1996).
 - [3] M. W. Richman, Acta Mech. **75**, 227 (1988); J. T. Jenkins, ASME J. Appl. Mech. **59**, 120 (1992).
 - [4] T. van Noije and M. Ernst, Gran. Matt. **1**, 52 (1998); S. Esipov and T. Pöschel, J. Stat. Phys. **86**, 1385 (1997).
 - [5] Y. Taguchi and H. Takayasu, Europhys. Lett. **30**, 499 (1995); A. Puglisi, V. Loreto, U. Marconi, A. Petri and A. Vulpiani, Phys. Rev. Lett. **81**, 3848 (1998).
 - [6] R. Cafiero, S. Luding and H. J. Herrmann, Phys. Rev. Lett. **84**, 6014 (2000); S. Moon, J. Swift, and H. L. Swinney, Phys. Rev. E **69**, 011301 (2004); J. van Zon and F. MacKintosh, Phys. Rev. Lett. **93**, 038001 (2004).
 - [7] F. Rouyer and N. Menon, Phys. Rev. Lett. **85**, 3676 (2000); W. Losert, D. Cooper, J. Delour, A. Kudroli, and J. P. Gollub, Chaos **9**, 682 (1999).
 - [8] D. Blair and A. Kudroli, Phys. Rev. E., **64**, 050301 (2001); G. Baxter and J. Olafsen, Nature **425**, 680 (2003).

- [9] S. Moka and P. R. Nott, Phys. Rev. Lett. **95**, 068003 (2005); V. Natarajan and M. Hunt, J. Fluid Mech. **304**, 1 (1995).
- [10] C. Denniston and H. Li, Phys. Rev. E **59**, 3289 (1999); E. Liss, S. Conway, and B. Glasser, Phys. Fluids **14**, 3309 (2002).
- [11] B. Lubachevsky, J. Comp. Phys. **94**, 255 (1991).
- [12] J.-C. Tsai, W. Losert, G. A. Voth, and J. P. Gollub, Phys. Rev. E **65**, 011306 (2001); K. C. Vijayakumar and M. Alam, *Manuscript in preparation* (2007).
- [13] Y. Murayama and M. Sano, J. Phys. Soc. Japan, **67**, 1826 (1998).